ACS APPLIED MATERIALS & INTERFACES

Research Article

www.acsami.org

Photoresponsive Coumarin-Tethered Multifunctional Magnetic Nanoparticles for Release of Anticancer Drug

S. Karthik,[†] Nagaprasad Puvvada,[†] B. N. Prashanth Kumar,[‡] Shashi Rajput,[‡] Amita Pathak,[†] Mahitosh Mandal,[‡] and N. D. Pradeep Singh*[,†]

[†]Department of Chemistry and [‡]School of Medical Science and Technology, Indian Institute of Technology Kharagpur, Kharagpur 721302, India

Supporting Information

ABSTRACT: Recently, photoresponsive nanoparticles have received significant attention because of their ability to provide spatial and temporal control over the drug release. In the present work, we report for the first time photoresponsive multifunctional magnetic nanoparticles (MNPs) fabricated using coumarin-based phototrigger and Fe/Si MNPs for controlled delivery of anticancer drug chlorambucil. Further, newly fabricated photoresponsive multifunctional MNPs were also explored for cell luminescence imaging. In vitro biological studies revealed that coumarin tethered Fe/Si MNPs of ∼9 nm size efficiently delivered the anticancer drug chlorambucil into cancer cells and thereby improving the drug action to kill the cancer cells upon irradiation. Such multifunctional MNPs with strong fluorescence, good biocompatibility and efficient photocontrolled drug release ability will be of great benefit in the construction of light-activated multifunctional nano drug delivery systems.

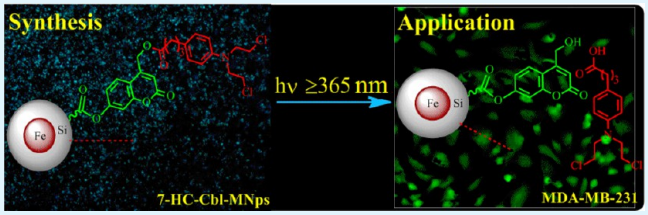

KEYWORDS: *phototrigger, magnetic nanoparticles, coumarin, drug delivery, chlorambucil*

INTRODUCTION

Multifunctional nano drug delivery systems (DDSs) have become current focus in the area of cancer treatments because of their unique ability to simultaneously perform fast diagnosis and provide efficient therapy.[1] A major goal in constructing multifunctional nano DDSs is to design multifunctional nanoparticles that will provide various functionalities including imaging, targeting, therapy, etc.[2] Several multifunctional nanoparticles have been prepared from various building blocks, such as organic (polymers, lipids, proteins, polysaccharides, etc.) and inorganic (iron, gold, silica, quantum dots, etc.) materials.[3−8] Among them magnetic nanoparticles (MNPs) have captured great attention for constructing multifunctional nanoparticles because of their unique properties like biocompatibility, intrinsic diagnostic ability to enhance MR contrast, magnetic responsiveness in the context of targeted drug delivery and facile surface modification.[9] Although, most of these multifunctional MNPs offer advantages in tumor targeting and multimodal imaging, still its application in drug delivery is restricted because of lack of precise control over the drug release.

Recently, photoresponsive nanoparticles have gained considerable importance in the area of DDSs for cancer therapy because of their key ability to regulate drug release spatially and temporally by external regulated light stimuli.[10,11] Generally, photoresponsive nanoparticles for DDSs are constructed using two main ingredients: biocompatible nanoparticles and "phototrigger".[12] Between them "phototriggers" are small organic molecules that perform two important functions (i) precise control over the drug release and (ii) as a linker between the nanoparticles and the drug.

Specific types of recently developed photoresponsive nanoparticles for DDSs include gold nanoparticles attached with phototrigger *o*-nitrobenzyl moiety,[13] mesoporous silica grafted with two-photon coumarin-based phototrigger,[14] photoresponsive block copolymer micelles constructed using phototrigger [7-(diethylamino)coumarin-4-yl]methyl,[15] and fluorescent organic nanoparticles based on perylen-3-ylmethanol chromophore.[16] Among the above-mentioned phototriggers, coumarin-based phototriggers have been extensively utilized in the construction of photoresponsive nanoparticles for DDS because of their strong fluorescence and efficient photorelease ability. Hence, we thought to construct for the first time photoresponsive nano DDSs using multifunctional Fe/Si MNPs as a nanocarrier and fluorescent 7-hydroxy coumarin as a phototrigger for both cell imaging and controlled delivery of anticancer drug chlorambucil.

EXPERIMENTAL SECTION

Materials. All reagents were purchased from Sigma Aldrich and used without further purification. Acetonitrile and dichloromethane were distilled from CaH_2 before use. ^1H NMR spectra were recorded on a BRUKER-AC 200 MHz spectrometer. Chemical shifts are reported in ppm from tetramethylsilane with the solvent resonance as

Received: March 24, 2013
Accepted: May 21, 2013
Published: May 21, 2013

   dx.doi.org/10.1021/am401059k | ACS Appl. Mater. Interfaces 2013, 5, 5232−5238

the internal standard (deuterochloroform: 7.26 ppm). Data are reported as follows: chemical shifts, multiplicity (s = singlet, d = doublet, t = triplet, m = multiplet), coupling constant (Hz). ^{13}C NMR (50 MHz) spectra were recorded on a BRUKER-AC 200 MHz Spectrometer with complete proton decoupling. Chemical shifts are reported in ppm from tetramethylsilane with the solvent resonance as the internal standard (deuterochloroform: 77.2 ppm). UV/vis absorption spectra were recorded on a Shimadzu UV-2450 UV/vis spectrophotometer, fluorescence emission spectra were recorded on a Hitachi F-7000 fluorescence spectrophotometer, FT-IR spectra were recorded on a Perkin-Elmer RXI spectrometer and HRMS spectra were recorded on a JEOL-AccuTOF JMS-T100L mass spectrometer. Transmission electron microscopy (TEM) was measured on a FEI Tecnai G220S-Twin at 200 kV. The TEM sample was prepared by dispersing compounds in water and dropping on the surface of a copper grid. The surface charge of the nanoparticles was investigated through zeta potential measurements (Zetasizer 4, Malvern Instruments, U.K.). DLS measurements were done using a Brookhaven 90 Plus particle size analyzer. Magnetic measurements were carried out using SQUID VSM DC magnetometer (Quantam Design, USA). Photolysis of all the ester conjugates were carried out using 125 W medium pressure Hg lamp supplied by SAIC (India). Chromatographic purification was done with 60−120 mesh silica gel (Merck). For reaction monitoring, precoated silica gel 60 F254 TLC sheets (Merck) were used. RP-HPLC was taken using mobile phase acetonitrile at a flow rate of 1 mL/min (detection: UV 254 nm).

Synthesis of Acid Functionalized Magnetic Nanoparticles (MNPs). The amine-functionalized magnetic nanoparticles were synthesized by using our previously reported procedure.[17] Amine functionalized magnetic nanoparticles were then treated with succinic anhydride and catalytic amount of triethyl amine in dry DMF and refluxed for 24 h to yield acid functionalized nanoparticles (Fe/Si MNPs), which were then recovered by applying an external magnetic field, washed several times with methanol, and dried in a vacuum oven at 50 °C.

Synthesis of Coumarin-Chlorambucil Conjugate (7-HC-Cbl). *i. Synthesis of Phototrigger 7-Hydroxy-4-bromomethyl Coumarin.* A mixture containing 1, 3-dihydroxybenzene (220 mg, 2 mmol), ethyl 4-bromoacetoacetate (420 mg, 2 mmol), and a catalytic amount of 70% H_2SO_4 was stirred at room temperature for 8 h. After addition of water (50 mL), the resulting precipitate was filtered off and dried under vacuum to afford the product 7-hydroxy-4-bromomethyl coumarin as pale yellow solid (85%).

ii. Synthesis of Coumarin−Chlorambucil Conjugate (7-HC-Cbl). Treatment of 7-hydroxy-4-bromomethyl coumarin (0.100 g, 0.29 mmol) with chlorambucil (0.088 g, 0.29 mmol) in the presence of potassium carbonate (0.048 g, 0.34 mmol) in dry *N*,*N*-dimethylformamide (DMF) at room temperature for a period of 6 h afforded the conjugate as a yellow solid. The crude conjugate was purified by column chromatography using 35% EtOAc in pet ether to give the coumarin−chlorambucil conjugate (70%). Yellow solid; TLC Rf 0.45 (35% EtOAc in pet ether); ^{1}H NMR ($CDCl_3$, 200 MHz): δ = 7.39 (d, J = 8.2 Hz, 1H), 7.09(d, J = 8.4 Hz, 2H), 6.85 (s, 2H), 6.64 (d, J = 8.4 Hz, 2H), 6.35 (s, 1H), 5.25 (s, 2H), 3.69−3.52 (m, 8H), 2.56−2.49 (t, J = 7.2 Hz, 2H), 2.43−2.36 (t, J = 7.4 Hz, 2H), 1.96−1.85 (m, 2H). ^{13}C NMR ($CDCl_3$, 50 MHz): δ = 173.6, 162.3, 155.3, 151.2, 145.3, 129.3, 126.3, 114.3, 113.7, 111.2, 109.7, 104.6, 64.6, 53.6, 40.6, 33.9, 33.7, 26.8. FTIR (KBr, cm^{-1}): 1715, 1619, 3200. UV−vis (EtOH): λmax (log ε): 320 (1.39). HRMS calcd For $C_{24}H_{25}Cl_2NO_5$ [MH$^+$], 477.1810; found, 477.1805.

Preparation of Drug-Loaded Fe/Si Magnetic Nanoparticles (7-HC-Cbl-MNPs). Acid-functionalized Fe/Si magnetic nanoparticles (100 mg) were dissolved in 1 mL of thionyl chloride and were stirred for 2 h at 60 °C. Then thionyl chloride was removed under vacuum to afford the acid chloride functionalized Fe/Si nanoparticles (**1**) as brown solid. Then the acid chloride functionalized Fe/Si nanoparticles (**1**) were dissolved in dry DCM (5 mL). To the solution **7-HC-Cbl** (0.100 g) was added followed by triethylamine (62 μL, 0.45 mmol). The mixture was stirred at room temperature for 1 h; the reaction was monitored using UV−vis absorption spectroscopy. After the completion of the reaction, the reaction mixture was centrifuged and 7-HC-Cbl-MNPs were collected.

Photoinduced Anticancer Drug Release by 7-HC-Cbl-MNPs. A suspension of 7-HC-Cbl-MNPs was prepared by dispersing 1 mg of nanoparticles in 1 mL of acetonitrile/water (9:1 v/v) mixture. Half of the solution was kept in dark and to the remaining half nitrogen was passed and irradiated by UV light (≥365 nm) using 125 W medium pressure Hg lamp with a suitable filter (1 M $CuSO_4$ solution in 0.1 N H_2SO_4). At regular time intervals, a small aliquot (100 μL) of the suspension was taken out and centrifuged (5000 r/min) for 10 min, the obtained transparent solution was analyzed by reversed-phase HPLC using mobile phase acetonitrile, at a flow rate of 1 mL/min.

Hydrolytic Stability Data of 7-HC-Cbl-MNPs in Dark Condition at Different pH Value. One milliliter of 2 × 10^{-4} M solution of 7-HC-Cbl-MNPs was added to PBS solutions (3 mL) of different pH values. Further to examine the hydrolytic stability of 7-HC-Cbl-MNPs at physiological pH (pH ∼ 7.4), 7-HC-Cbl-MNPs was added to PBS containing 10% fetal bovine serum. All the tubes were kept in ultrasonic for 10 min to make the solutions homogeneous and stored at 37 °C in dark condition for 48 h. Then 2 mL of acetonitrile was added to all the tubes and ultrasonicated for 10 min. All the solutions were then centrifuged and the supernatant liquids analyzed by reverse phase HPLC to examine the remaining percentage of the 7-HC-Cbl-MNPs.

Cell Imaging and in Vitro Cytotoxicity Studies of 7-HC-Cbl-MNPs Using MDA-MB-231 Breast Cancer Cell Line. *a. Cellular Localization of 7-HC-Cbl-MNPs.* To study the cellular localization of 7-HC-Cbl-MNPs, we seeded MDA-MB-231 cells at a density of 3 × 10^4 on sterile glass coverslips, respectively. The coverslips were pretreated with 0.01% poly-L-lysine before seeding. The cells were then incubated with 250 μg/mL of 7-HC-Cbl-MNPs in cell culture medium for 3, 6, and 12 h at 37 °C and 5%CO_2. After incubation, the coverslips were removed and washed twice with PBS solution. Then cells were fixed using 3.7% paraformaldehyde for 20 min and washed two times with PBS. Imaging was analyzed using fluorescence microscopy.

b. In Vitro Cytotoxicity Study of 7-HC-Cbl-MNPs Using MDA-MB-231 Cell Line. I. Before Irradiation. The cytotoxicity of 7-HC-Cbl-MNPs was studied using MTT assay. Cytotoxicity of chlorambucil, Fe/Si MNPs and 7-HC-Cbl-MNPs was determined with and without irradiation of UV light on MDA-MB-231 breast cancer cells. Cells in their exponential growth phase were trypsinized and seeded in 96-well flat-bottom culture plates at a density of 1 × 10^4 cells per well in 100 μL of complete Dulbecco's modified eagle's medium (DMEM). The cells were allowed to adhere and grow for 24 h at 37 °C in an incubator in presence of 5% CO_2 and then the medium was replaced with 100 μL fresh incomplete DMEM medium containing different concentrations of chlorambucil, Fe/Si MNPs and 7-HC-Cbl-MNPs (0−110 μM). The cells were then incubated for 48 h at 37 °C in 5% CO_2. Thereafter, fresh media containing 0.40 mg/mL MTT were added to the 95-well plates and incubated for 4 h at 37 °C in 5% CO_2. Formazan crystals thus formed were dissolved in DMSO after decanting the earlier media and absorbance recorded at 595 nm. Percentage of cytotoxicity was plotted against concentration of substrate.

ii. After Irradiation. MDA-MB-231 maintained in minimum essential medium (in 96-well cell-culture plate at concentration of 1 × 10^4 cells/mL) containing 10% fetal bovine serum (FBS) and different concentrations of chlorambucil, Fe/Si MNPs and 7-HC-Cbl-MNPs (0−110 μM) was incubated for 4 h at 37 °C and 5% CO_2. Then the cells were irradiated by UV light (≥365 nm) for 30 min (keeping the cell-culture plate 5 cm apart from the light source) using 125 W medium pressure Hg lamp with 1 M $CuSO_4$ solution as UV cutoff filter. After irradiation the cells were again incubated for 48 h. Then cytotoxicity was measured using the MTT assay as described in section b.i.

c. Cell Cycle Analysis. MDA-MB-231 breast cancer cells were cultured in 60 mm petridishes for 24 h at 37 °C in 5% CO_2 a density of 1 × 10^5 and then treated with IC_{50} concentration of Fe/Si MNPs, chlorambucil, and 7-HC-Cbl-MNPs and the cells were incubated for

Scheme 1. Preparation of Coumarin-Chlorambucil Loaded Fe/Si Magnetic Nanoparticles (7-HC-Cbl-MNPs)

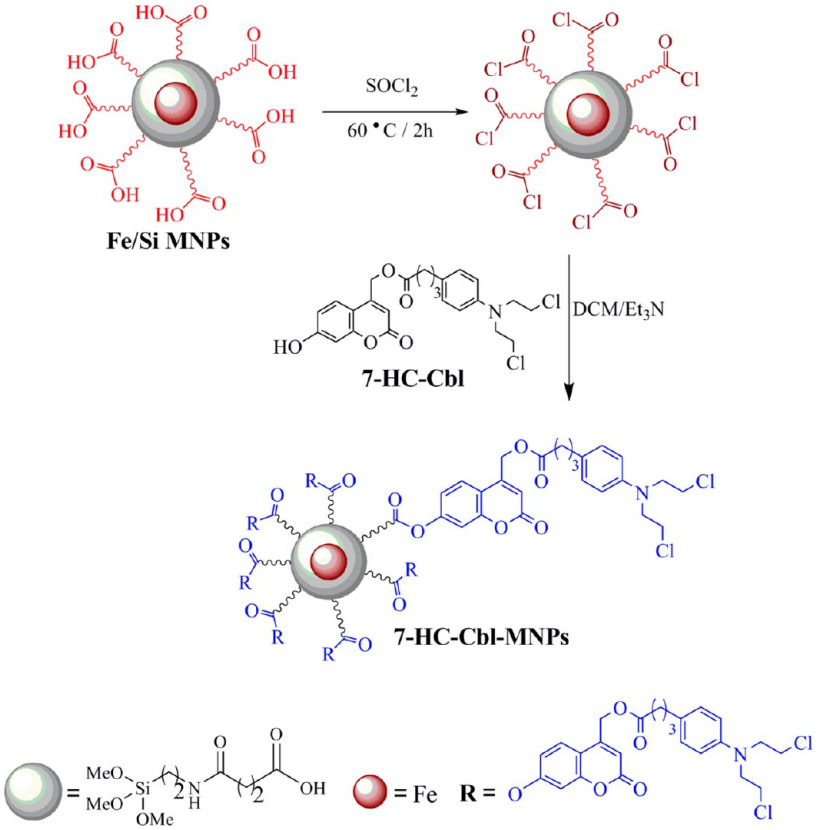

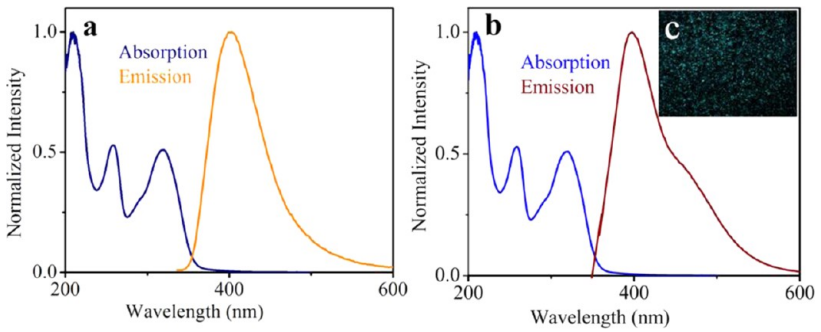

Figure 1. (a) Normalized absorption and emission spectra of 7HC-Cbl conjugate in water. (b) Normalized absorption and emission spectra of 7HC-Cbl-MNPs in water. (C) Confocal laser scanning microscopy (CLSM) image of the 7-HC-Cbl-MNPs.

12 h at 37 °C under 5% CO_2. In this study, untreated and Fe/Si MNPs treated cells were used as reference control. Chemically treated cells were irradiated for 30 min by UV light (≥365 nm) for 30 min (keeping the cell-culture plate 5 cm apart from the light source) using 125 W medium pressure Hg lamp with 1 M $CuSO_4$ solution as UV cutoff filter. After irradiation the cells were again incubated for 48 h at 37 °C under 5% CO_2. After incubation, cells were trypsinized and centrifuged at 1200 rpm for 5 min at 4 °C. The pellet was suspended in 10 mL of PBS and then centrifuged at 1300 rpm for 10 min at 4 °C. The supernatant was discarded and the pellet was fixed with 2 mL of ice-cold ethanol solution (70% v/v in PBS) at 4 °C overnight. Fixed cells were centrifuged at 1300 rpm for 10 min at 4 °C and the pellet was incubated with PI mixture (10 mg/mL RNase, 20 mg/mL propidium iodide dissolved in cold PBS) for 30 min at 37 °C. DNA content analysis was carried out on a FACS Calibur (BD Bioscience, USA) flow cytometer (10,000 events were acquired for each sample). The data obtained were processed for cell cycle analysis with the cell quest pro software package. The amount of propidium iodide intercalating to DNA was used as the parameter to determine the cell cycle distribution phases. Apoptosis fraction was considered as DNA loss resulting in a sub-G1 peak.

RESULTS AND DISCUSSION

Preparation of Coumarin−Chlorambucil Tethered Fe/Si Magnetic Nanoparticles (7-HC-Cbl-MNPs). We synthesized coumarin−chlorambucil conjugate (7-HC-Cbl), by treating 7-hydroxy-4-bromomethylcoumarin with chlorambucil in presence of potassium carbonate in dry DMF at room temperature (see Scheme S1 in the Supporting Information). On the other hand, acid chloride functionalized Fe/Si MNPs were prepared from their corresponding carboxylic-acid-functionalized Fe/Si MNPs by treatment with thionyl chloride. Finally, coumarin−chlorambucil tethered Fe/Si magnetic nanoparticles (7-HC-Cbl-MNPs) was constructed by reacting coumarin−chlorambucil conjugate (7-HC-Cbl) with freshly prepared acid chloride-functionalized Fe/Si MNPs in the

dx.doi.org/10.1021/am401059k | ACS Appl. Mater. Interfaces 2013, 5, 5232−5238

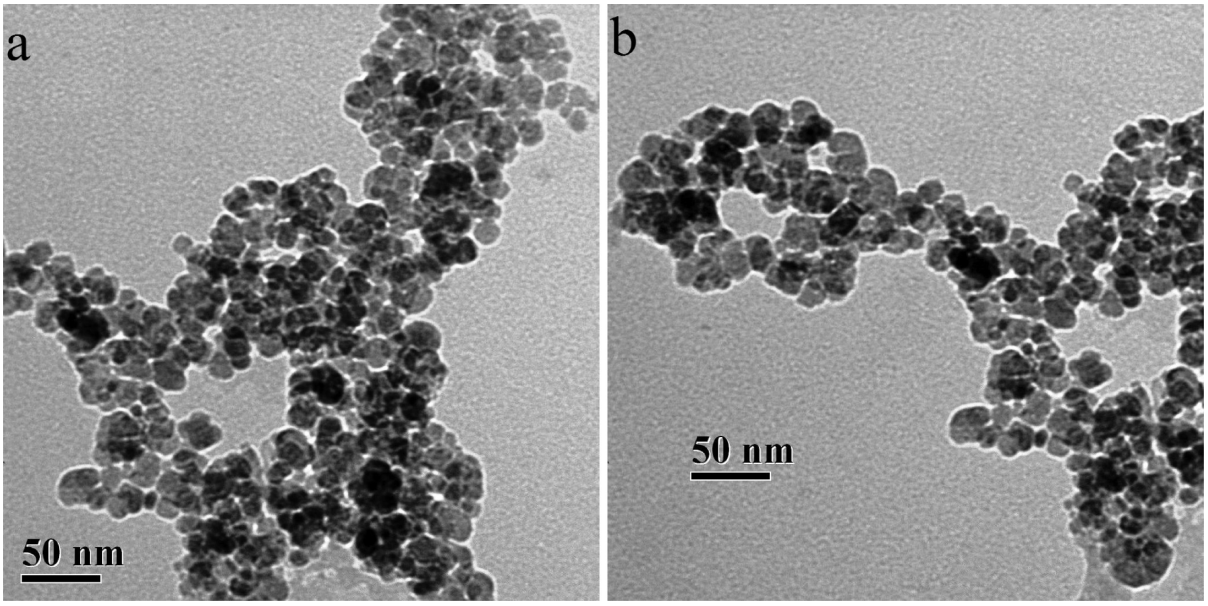

Figure 2. (a, b) TEM images: (a) 7-HC-Cbl-MNPs, (b) Fe/Si MNPs.

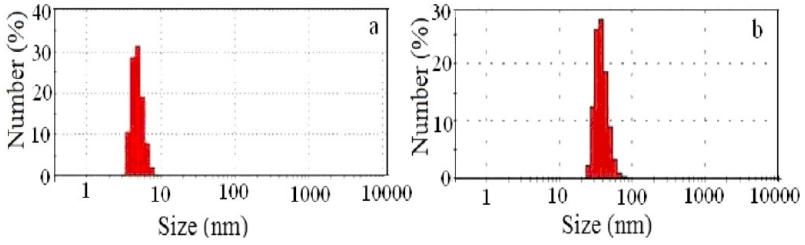

Figure 3. Dynamic light scattering spectra of 7-HC-Cbl-MNPs in water: (a) 7-HC-Cbl-MNPs and (b) Fe/Si MNPs.

presence of triethyl amine in dry DCM at room temperature (Scheme 1).

Physicochemical Properties of Photoresponsive Multifunctional Magnetic Nanoparticles (7-HC-Cbl-MNPs). *FTIR, UV–Visible and Fluorescence Spectral Analysis.* The attachment of 7-HC-Cbl on the surface of Fe/Si MNPs was analyzed by FT-IR, UV–vis, and fluorescence spectroscopic methods. The FT-IR spectra of acid functionalized Fe/Si MNPs showed peaks at 3636, 1669, 1010, 2870, and 608 cm−1, which correspond to acid O–H bending, C═O stretching, Si–O–Si bond stretching, C–H bond vibration, and Fe–O bond vibration, respectively, demonstrating the acidsilane modification on Fe_3O_4 nanoparticles (see Figure S1 in the Supporting Information). After treatment with the coumarin-chlorambucil, Fe/Si MNPs showed band at 1669 cm^{-1} corresponding to C═O stretching of coumarin cyclic ester and new ester linkage band around 1640 cm^{-1}. Additionally, characteristic peaks for the Fe–O, Si–O–Si were also observed at 608, 1010 cm−1 confirming the successful loading of coumarin-chlorambucil on Fe_3O_4 nanoparticles.

The UV–vis and fluorescence spectra of 7-HC-Cbl conjugate and 7-HC-Cbl-MNPs are presented in Figure 1. 7-HC-Cbl conjugate showed two absorption peaks at 250 and 340 nm due to n–π^* and π–π^* transitions, respectively, and strong emission peak at 420 nm (Figure 1a).[17] On the other hand, 7-HC-Cbl-MNPs showed similar absorption and emission peaks compared to 7-HC-Cbl conjugate, except with slight shift in their absorption and emission maxima, convincing that the coumarin–chlorambucil was successfully conjugated on Fe_3O_4 nanoparticles (Figure 1b). Further, confocal laser scanning microscopy (CLSM) fluorescent images of 7-HC-Cbl-MNPs showed successful preparation of 7-HC-Cbl-MNPs (Figure 1c). The above UV–vis and fluorescence spectral studies indicate that our 7-HC-Cbl-MNPs can be used both for cell imaging and release of the anticancer drug using UV irradiation above 365 nm. The loading efficiency of 7-HC-Cbl on the surface of Fe/Si MNPs was determined to be approximately 80 ng in 1 mg of nanoparticles by UV–vis spectroscopy (see Figure S2 in the Supporting Information).

TEM Study. The size and shape of magnetic nanoparticles were observed by the TEM study. The representative TEM images of 7-HC-Cbl-MNPs and Fe/Si MNPs are presented in Figure 2. Figure 2a shows that the 7-HC-Cbl-MNPs were well-dispersed and globular in nature with an average particle size of 9 nm. This size of the nanoparticles is well within the preferred range of the nanoparticles useful for effective drug-delivery.[18]

DLS and Zetapotential Measurements of Fe/Si MNPs and 7-HC-Cbl-MNPs. The Fe/Si MNPs and 7-HC-Cbl-MNPs was dispersed in water and used for DLS measurement. The DLS data shows that Fe/Si MNPs and 7-HC-Cbl-MNPs were ∼60 and ∼9 nm, respectively (Figure 3). The increase in particle size of Fe/Si MNPs compared to 7-HC-Cbl-MNPs implies that nanoparticles are highly agglomerated in the medium because of earth magnetic field.

The zeta potentials values for Fe/Si MNPs and 7-HC-Cbl-MNPs are shown in Figure 4a. The negative potential for Fe/Si MNPs implies that free carboxylic acid groups are present on the surface of MNPs. On the other hand, 7-HC-Cbl-MNPs

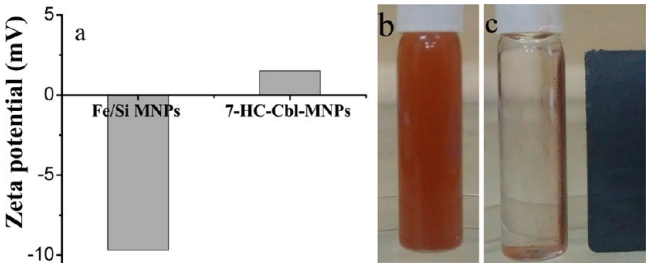

Figure 4. (a) Zeta potential profile of Fe/Si MNPs and 7-HC-Cbl-MNPs. (b, c) Two vials containing 7-HC-Cbl-MNPs in aqueous solutions (b) without and (c) with an external magnetic field.

displayed positive zeta potential indicating that free acid groups on the surface of Fe/Si MNPs were functionalized by coumarin−chlorambucil conjugate. Thus 7-HC-Cbl-MNPs having positive zeta potential on the surface can be effectively internalized into the cells.

Magnetic Properties of 7-HC-Cbl-MNPs and Fe/Si MNPs. The magnetic measurements of Fe/Si MNPs and 7-HC-Cbl-MNPs have been performed at room temperature with superconducting quantum interference device (SQUID) and their results are depicted in Figure S4 in the Supporting Information. The prepared samples did not show any remanence and hysteresis, signifying their super paramagnetic nature. Saturation magnetization values for Fe/Si MNPs and 7-HC-Cbl-MNPs were found to be 71.2 and 65.2 emu g^{-1}, respectively. A decrease in the magnetic saturation value in the drug-loaded Fe/Si MNPs can be attributed to the presence of surface functional groups. Further to demonstrate that 7-HC-Cbl-MNPs could be targeted to any specific site of interest by applying external magnetic field, we taken 7-HC-Cbl-MNPs dispersed in aqueous solution in two different vials. As illustrated in Figure 4b, c, the dispersed nanoparticles of the vial placed close to magnet were found to be attracted to the walls of the vial.[19]

Hydrolytic Stability of 7-HC-Cbl-MNPs at Different pH Values. To check the hydrolytic stability of 7-HC-Cbl-MNPs, 3 mL of phosphate buffer containing 2×10^{-4} M of 7-HC-Cbl-MNPs at different pH values (5.6, 7.4 and 8) was prepared separately. On the other hand, similar concentration of 7-HC-Cbl-MNPs in PBS containing 10% fetal bovine serum (pH ~7.4) was also prepared to monitor the stability of 7-HC-Cbl-MNPs under biological environment. All the tubes were kept in ultrasonic for 10 min to make the solutions homogeneous and stored at 37 °C in dark condition for 72 h. Then 2 mL of acetonitrile was added to all the tubes and was ultrasonicated for 10 min. Then all the solutions were centrifuged and the supernatant liquid were analyzed by reverse phase HPLC. We observed insignificant (2−3%) decomposition (Table 1), which proves that the 7-HC-Cbl-MNPs are quite stable in the dark.

Photoinduced Release of Chlorambucil from 7-HC-Cbl-MNPs. A suspension of 7-HC-Cbl-MNPs (1×10^{-4} M) in acetonitrile: water (9:1) was irradiated by UV light (≥365 nm) using 125 W medium pressure Hg lamp with a suitable filter (1 M $CuSO_4$ solution in 0.1 N H_2SO_4). The course of the photorelease of chlorambucil was followed by reverse phase HPLC using acetonitrile as the mobile phase keeping the flow rate of 1 mL/min. The HPLC profile indicates about 90% of the loaded anticancer drug (chlorambucil) was effectively released within 30 min of photolysis (Figure 5). Further, we

Table 1. Remaining Percentage of 7-HC-Cbl-MNPs in Dark Conditions at Different pH Values

		% of 7-HC-Cbl-MNPs depleted			
photoresponsive nanocarrier	time (day)	(pH 5.6) PBS	(pH 7.4) PBS	(pH 8) PBS	(pH 7.4) FBS
7-HC-Cbl-MNPs	2	2	2	3	2

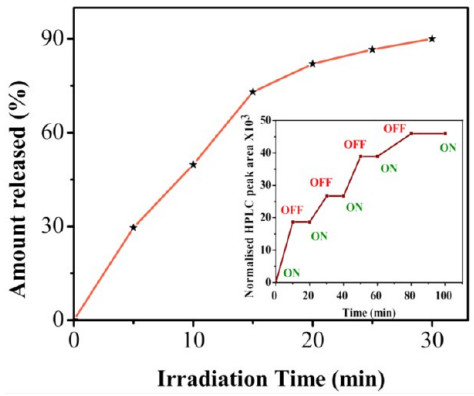

Figure 5. Percentage of chlorambucil released from 7-HC-Cbl-MNPs. Inset is the partial progress for the release of chlorambucil under bright and dark conditions. "ON" indicates the beginning of light irradiation; "OFF" indicates the ending of light irradiation.

also demonstrated precise control of the photolytic release of chlorambucil by monitoring the release of chlorambucil after periods of exposure to light and dark condition. The Figure 5 inset clearly shows that the drug release proceeded only under illumination.

Cellular Localization 7-HC-Cbl-MNPs. To establish 7-HC-Cbl-MNPs can be used as versatile photoresponsive nano DDSs, we studied cellular uptake efficiency of drug-loaded MNPs (7-HC-Cbl-MNPs) by MDA-MB-231 cells at different time periods using fluorescence microscopy (Figure 6). After 3 h of incubation with 7-HC-Cbl-MNPs, cells showed green fluorescence and aggregation of nanoparticles in the cytoplasm. Further increase in fluorescence and nanoparticle accumulation in MDA-MB-231 cells was observed as incubation time increased to 6 h.

Anticancer Efficacy of 7-HC-Cbl-MNPs before and after Photolysis. Cell viability was evaluated using MTT assay in breast cancer cell MDA-MB-231.[20,21] Cells were incubated with chlorambucil, chlorambucil-loaded MNPs (7-HC-Cbl-MNPs), and Fe/Si MNPs for 4 h over a range of concentrations between 0 and 110 μM. After incubation, the cells were irradiated for 30 min under UV light (≥365 nm) and further incubated for 48 h. Cell viability of 35% was observed with free chlorambucil at the concentration of 110 μM. For the same concentration of loaded chlorambucil on MNPs (7-HC-Cbl-MNPs) the cell viability greatly reduced to 10%, which can be due to the efficient photorelease of anticancer drug chlroambucil inside the cancerous cell. On the other hand, cell viability was found to be largely unaffected by drug-free Fe/Si MNPs, indicating the cytotoxicity was likely caused by the released drug chlorambucil, upon light irradiation. Additionally, results of MTT assays also revealed a concentration-dependent decrease of cell viability for both free chlorambucil and 7-HC-Cbl-MNPs. It was noted that IC_{50} values of MDA-MB-231 cells decreased from 67.38 ± 1.45 μM for chlorambucil to 53.84 ±

dx.doi.org/10.1021/am401059k | ACS Appl. Mater. Interfaces 2013, 5, 5232−5238

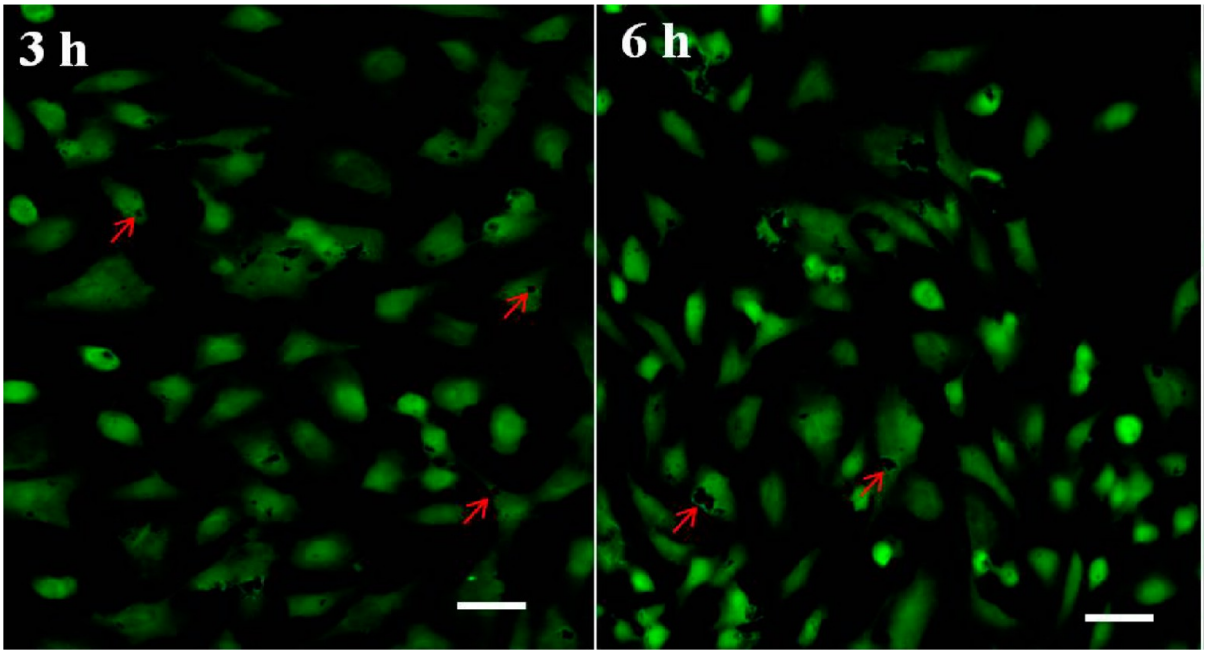

Figure 6. Cellular uptake of 7-HC-Cbl-MNPs by MDA-MB-231 cells at varying time intervals (scale bars: 3 and 6 h = 20 μm at 20× and 12 h = 40 μm at 40×); the nanoparticles are internalized by cell membrane and uniformly distributed in the cytoplasm (red arrows).

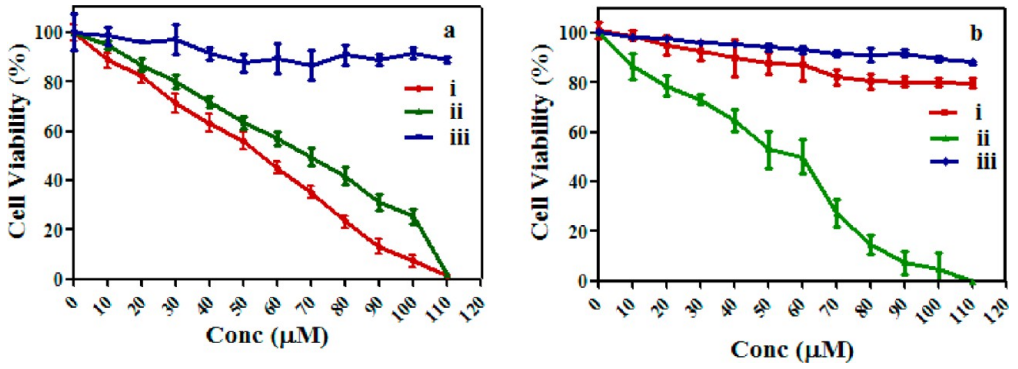

Figure 7. (a) Antiproliferative effect of chlorambucil on MDA-MB-231 cells incubated for 48h after 30 min of irradiation (i) 7-HC-Cbl-MNPs, (ii) chlorambucil, and (iii) drug-free Fe/Si MNPs. (b) Antiproliferative effect of chlorambucil on MDA-MB-231 cells incubated for 48 h, without irradiation, (i) 7-HC-Cbl-MNPs (ii) chlorambucil, and (iii) drug-free Fe/Si MNPs.

1.12 μM for the 7-HC-Cbl-MNPs (Figure 7a). 7-HC-Cbl-MNPs showed an increasing cytotoxicity to cancer cells.

The cytotoxic assay of chlorambucil, chlorambucil-loaded MNPs (7-HC-Cbl-MNPs) and Fe/Si MNPs were also performed on MDA-MB-231 cells without irradiation. Results showed 82% and 90% of cell viability at higher concentrations of chlorambucil-loaded MNPs (7-HC-Cbl-MNPs) and drug-free MNPs, respectively. However, cells treated with chlorambucil showed increasing cytotoxicity with rising drug concentration, having an IC_{50} at 70.52 ± 0.96 μM (Figure 7b). On comparison with the same concentration of free chlorambucil to that of loaded chlorambucil on MNPs, chlorambucil loaded on MNPs showed much lower cytotoxicity compared to free chlorambucil. But upon irradiation, chlorambucil loaded on MNPs showed an increasing cytotoxicity to cancer cells.

Cell Cycle Analysis by Flow Cytometer. Chlorambucil-induced apoptosis in MDA-MB-231 cells was also demonstrated by cell cycle analysis. The percentage of apoptotic cells was counted using a FACs Calibur flow cytometer. As shown in Figure S5 in the Supporting Information, 2.93 ± 0.56% apoptosis was found for untreated control cells, whereas cells treated with Fe/Si-MNPs, chlorambucil, and 7-HC-Cbl-MNPs had 4.37 ± 0.83%, 25.05 ± 0.17%, and 30.21 ± 0.24% of apoptosis, respectively, at 48 h after treatment to UV light for 30 min. It is evident that free chlorambucil and 7-HC-Cbl-MNPs induced more apoptosis than Fe/Si MNPs. The higher apoptotic activity of 7-HC-Cbl-MNPs than free chlorambucil suggests that chlorambucil-loaded magnetic nanoparticles can significantly enhance the efficiency of the intracellular delivery and slow release of chlorambucil for sustained period of time.

CONCLUSION

In summary, we have developed an excellent photoresponsive multifunctional DDS based on Fe/Si MNPs and coumarin phototrigger for cell imaging and photocontrolled delivery of anticancer drug. The strong fluorescence of 7-HC-Cbl-MNPs has been explored for the in vitro cellular imaging application. Photocontrolled drug release ability of 7-HC-Cbl-MNPs has been established by the means of periodic exposure to light and

dx.doi.org/10.1021/am401059k | ACS Appl. Mater. Interfaces 2013, 5, 5232−5238

dark condition. Interestingly, 7-HC-Cbl-MNPs showed good biocompatibility, cellular uptake property and precise control over the drug release to kill the cancer cells upon irradiation. Thus, we except the above study may be a promising starting point for the use of photoresponsive MNPs in the construction of multifunctional targeted drug delivery systems with precise control over the drug release.

■ ASSOCIATED CONTENT

Supporting Information

^{1}H and ^{13}C NMR spectra, FT-IR, loading of 7-HC-Cbl on Fe/Si MNPs, fluorescent spectra of 7-HC-Cbl-MNPs and 7-HC-Cbl, confocal image of 7-HC-Cbl-MNPs, M-H curve of MNPs, and cell cycle analysis. This material is available free of charge via the Internet at http://pubs.acs.org.

■ AUTHOR INFORMATION

Corresponding Author

*E-mail: ndpradeep@chem.iitkgp.ernet.in.

Notes

The authors declare no competing financial interest.

■ ACKNOWLEDGMENTS

We thank DST (SERB) for financial support, DST-FIST for 400 MHz NMR. S.K. is thankful to Indian Institute of Technology Kharagpur for the fellowship.

■ ABBREVIATIONS

(MNPs), magnetic nanoparticles
(DDSs), drug delivery systems
(7-HC-Cbl), 7-hydroxy-coumarin chlorambucil
(7-HC-Cbl-MNPs), 7-HC-Cbl-loaded Fe/Si magnetic nanoparticles

■ REFERENCES

(1) Voliani, V.; Signore, G.; Nifosí, R.; Ricci, F.; Luin, S.; Beltram, F. *Recent Patents on Nanomedicine* **2012**, *2*, 1−11.
(2) Kim, D, K.; Dobson, J. *J. Mater. Chem* **2009**, *19*, 6294−6307.
(3) Torchilin, V. P. *Pharm. Res.* **2007**, *24*, 1−16. Savic, R.; Luo, L.; Eisenberg, A.; Maysinger, D. M. *Science* **2003**, *300*, 615−618. Min, K. H.; Kim, J. H.; Bae, S. M.; Shin, H.; Kim, M. S.; Park, S.; Lee, H.; Park, R. W.; Kim, I. S.; Kim, K.; Kwon, I. C.; Jeong, S. Y.; Lee, D. S. *J. Controlled Release* **2010**, *144*, 259−266. Koo, H.; Lee, H.; Lee, S.; Min, K. H.; Kim, M. S.; Lee, D. S.; Choi, Y.; Kwon, I. C.; Kim, K.; Jeong, S. Y. *Chem. Commun.* **2010**, *46*, 5668−5670.
(4) Kim, J.; Piao, Y.; Hyeon, T. *Chem. Soc. Rev* **2009**, *38*, 372−390. Jun, Y. W.; Lee, J. H.; Cheon, J. *Angew. Chem., Int. Ed* **2008**, *47*, 5122−5135.
(5) Lee, S.; Cha, E.-J.; Park, K.; Lee, S. Y.; Hong, J. K.; Sun, I. C.; Kim, S. Y.; Choi, K.; Kwon, I. C.; Kim, K.; Ahn, C. H. *Angew. Chem. Int. Ed* **2008**, *47*, 2804−2807. Qian, X. M.; Nie, S. M. *Chem. Soc. Rev* **2008**, *37*, 912−920. Huang, X. H.; El-Sayed, I. H.; Qian, W.; El-Sayed, M. A. *J. Am. Chem. Soc.* **2006**, *128*, 2115−2120. Sun, I. C.; Eun, D. K.; Koo, H.; Ko, C. Y.; Kim, H. S.; Yi, D. K.; Choi, K.; Kwon, I. C.; Kim, K.; Ahn, C. H. *Angew. Chem., Int. Ed* **2011**, *50*, 9348−9351.
(6) Ji, S.R..; Liu, C.; Zhang, B.; Yang, F.; Xu, J.; Long, J.; Jin, C.; Fu, D.l.; Ni, Q.x.; Yu, X.j. *Biochim. Biophys. Acta, Rev. Cancer* **2010**, *1806*, 29−35. De La Zerda, A.; Zavaleta, C.; Keren, S.; Vaithilingam, S.; Bodapati, S.; Liu, Z.; Levi, J.; Smith, B. R..; Ma, T. J.; Oralkan, O.; Cheng, Z.; Chen, X.; Dai, H.; Khuri-Yakub, B. T.; Gambhir, S. S. *Nat. Nanotechnol.* **2008**, *3*, 557−562. Kam, N. W. S.; O'Connell, M.; Wisdom, J. A.; Dai, H. *Proc. Natl. Acad. Sci. U.S.A.* **2005**, *102*, 11600−11605.
(7) Tanaka, K.; Kitamura, N.; Chujo, Y. *Bioconjugate Chem.* **2011**, *22*, 1484−1490. Benezra, M.; Penate-Medina, O.; Zanzonico, P. B.; Schaer, D.; Ow, H.; Burns, A.; DeStanchina, E.; Longo, V.; Herz, E.; Iyer, S.; Wolchok, J.; Larson, S. M.; Wiesner, U.; Bradbury, M. S. *J. Clin. Invest.* **2011**, *121*, 2768−2780.
(8) Lee, D.-E.; Koo, Z. H.; Sun, Z, I-C.; Ryu, J,H.; Kim, K.; Kwon, I, C. *Chem. Soc. Rev.* **2012**, *41*, 2656−2672.
(9) Yoon, T. J.; Kim, J. S.; Kim, B. G.; Yu, K. N.; Cho, M. H.; Lee, J. K. *Angew. Chem., Int. Ed* **2005**, *44*, 1068−1071.
(10) Yavuz, M. S.; Cheng, Y.; Chen, J.; Cobley, C. M.; Zhang, Q.; Rycenga, M.; Xie, J.; Kim, C.; Song, K. H.; Schwartz, A. G.; Wang, L. V.; Xia, Y. *Nat. Mater.* **2009**, *8*, 935−939. Heo, D. N.; Yang, D. H.; Moon, H.-J.; Lee, J. B.; Bae, M. S.; Lee, S. C.; Lee, W. J.; Sun, I.-C.; Kwon, I. K. *Biomaterials* **2012**, *33*, 989−998.
(11) Allen, T. M.; R. Cullis, P. *Science* **2004**, *303*, 1818−1822. Knežević, N. Ž.; Victor, S.-Y. L. *Nanoscale* **2013**, *5*, 1544−1551.
(12) Lin, Q.; Bao, C.; Fan, G.; Cheng, S.; Liu, H.; Liu, Z.; Zhu, L. *J. Mater. Chem* **2012**, *22*, 6680−6688.
(13) Agasti, S. S.; Chompoosor, A.; You, C.; Ghosh, P.; Kim, C. K.; Rotello, V. M. *J. Am. Chem. Soc.* **2009**, *131*, 5728−5729.
(14) Lin, Q.; Huang, Q.; Li, C.; Bao, C.; Liu, Z.; Li, F.; Zhu, L. *J. Am. Chem. Soc.* **2010**, *132*, 10645−10647.
(15) Babin, J.; Pelletier, M.; Lepage, M.; Allard, J.; Morris, D.; Zhao, Y. *Angew. Chem., Int. Ed.* **2009**, *48*, 3329−3332.
(16) Jana, A.; Sanjana, P, D, K.; Maiti, T, K.; Pradeep Singh, N, D. *J. Am. Chem. Soc.* **2012**, *134*, 7656−7659.
(17) Puvvada, N.; Mandal, D.; Panigrahi, P, K.; Pathak, A. *Toxicol. Res* **2012**, *1*, 196−200. Atta, S.; Jana, A.; Rajakumar, A.; Singh, P. N. D. *J. Agric. Food Chem.* **2010**, *58*, 11844−11851.
(18) Faraji, A. H.; Wipf, P. *Bioorg. Med. Chem.* **2009**, *17*, 2950−2962.
(19) Wang, Y.; Bin Li; Zhang, L.; Song, H.; Zhang, L. *ACS Appl. Mater. Interfaces* **2013**, *5*, 11−15.
(20) Venkatesan, P.; Puvvada, N.; Dash, R.; Prashanth Kumar, B. N.; Sarkar, D.; Azab, B.; Pathak, A.; Kundu, S. C.; Fisher, P. B.; Mandal, M . *Biomaterials* **2011**, *32*, 3794−3806.
(21) Venkatesan, P.; Mandal, M. *Cancer Nanotechnol.* **2011**, *2*, 67−79.